Enhancer control of *V(D)J* recombination at the TCRβ locus: differential effects on DNA cleavage and joining

William M. Hempel,[1,3] Patricia Stanhope-Baker,[2,3] Noëlle Mathieu,[1] Fang Huang,[1] Mark S. Schlissel,[2,4] and Pierre Ferrier[1,4]

[1]Centre d'Immunologie Institut National de la Santé et de la Recherche Médicale–Centre National de la Recherche Scientifique (INSERM-CNRS) de Marseille-Luminy, Marseille Cedex 9, France; [2]Department of Medicine, Department of Molecular Biology and Genetics, The Johns Hopkins University School of Medicine, Baltimore, Maryland 21205 USA

Deletion of the TCRβ transcriptional enhancer (Eβ) results in nearly complete inhibition of *V(D)J* recombination at the TCRβ locus and a block in αβ T cell development. This result, along with previous work from many laboratories, has led to the hypothesis that transcriptional enhancers affect *V(D)J* recombination by regulating the accessibility of the locus to the recombinase. Here we test this hypothesis by performing a detailed analysis of the recombination defect in Eβ-deleted ($E\beta^{-/-}$) mice using assays that detect various reaction intermediates and products. We found double-strand DNA breaks at recombination signal sequences flanking *D*β and *J*β gene segments in $E\beta^{-/-}$ thymuses at about one-third to one-thirtieth the level found in thymuses with an unaltered TCRβ locus. These sites are also subject to in vitro cleavage by the *V(D)J* recombinase in both $E\beta^{-/-}$ and $E\beta^{+/+}$ thymocyte nuclei. However, the corresponding *D*β-to-*J*β coding joints are further reduced (by 100- to 300-fold) in $E\beta^{-/-}$ thymuses. Formation of extrachromosomal *D*β-to-*J*β signal joints appears to be intermediately affected and nonstandard *D*β-to-*D*β joining occurs at the Eβ-deleted alleles. These data indicate that, unexpectedly, loss of accessibility alone cannot explain the loss of TCRβ recombination in the absence of the Eβ element and suggest an additional function for Eβ in the process of DNA repair at specific TCRβ sites during the late phase of the recombination reaction.

[*Key Words: V(D)J* recombination; TCRβ enhancer; RSS accessibility; double-strand break repair]

Received January 27, 1998; revised version accepted June 3, 1998.

V(D)J recombination, the only site-specific DNA rearrangement process known to occur in vertebrates, is required for the assembly of immunoglobulin and T cell receptor (TCR) genes and normal lymphocyte differentiation (for review, see Alt et al. 1992; Schatz et al. 1992; Lewis 1994; Bogue and Roth 1996). This process utilizes an enzyme complex, called the *V(D)J* recombinase, which targets conserved recombination signal sequences (RSSs) associated with all rearranging immunoglobulin and TCR *V*, *D*, and *J* gene segments. RSSs consist of conserved 7- and 9-nucleotide sequences (the heptamer and nonamer) separated by a 12- or 23- nucleotide spacer of nonconserved sequence. In vitro studies have demonstrated that two lymphoid-specific components of the recombinase, RAG1 and RAG2, are sufficient for recognition and double-strand cleavage of pairs of RSSs (for review, see Gellert 1997; Schatz 1997). Subsequent processing and joining of the cleaved intermediates require the additional activities of several factors involved in general DNA double-stranded break (DSB) repair (for review, see Weaver 1995; Lieber et al. 1997). In vivo, *V(D)J* recombination at endogenous immunoglobulin and TCR loci is tightly regulated with respect to cell lineage, stage of cell differentiation and, at particular gene segments and/or loci, allele usage (for review, see Willerford et al. 1996; Papavasiliou et al. 1997). Given that a common recombinase mediates all immunoglobulin and TCR gene rearrangements, it is assumed that these levels of regulation are imposed by changes in chromatin structure that affect the ability of particular gene segments to serve as a substrate, a concept known as recombinational accessibility (Alt et al. 1987; for review, see Sleckman et al. 1996; Schlissel and Stanhope-Baker 1997). However, neither the nature of the putative structural changes, nor the precise mechanism by which they are established, is known.

The DNA cleavage activity of the *V(D)J* recombinase occurs precisely at the junction between an RSS and the adjacent coding sequence, yielding a covalently closed hairpin end containing the coding gene segment (called a coding end, CE) and a blunt, 5′ phosphorylated end con-

[3]These authors contributed equally to this work.
[4]Corresponding authors.
E-MAIL mss@welchlink.welch.jhu.edu; FAX (410) 955-0964.
E-MAIL ferrier@ciml.univ.mrs.fr; FAX (33) 491-269430.

taining the RSS (called a signal end, SE) (for review, see Gellert 1997; Schatz 1997). Cleavage is biased toward RSS pairs with spacers of dissimilar lengths (coupled cleavage; Eastman et al. 1996; Van Gent et al. 1996; Steen et al. 1996). Following cleavage, the two resulting CEs are rapidly processed (involving opening of the hairpin ends and frequently deletion and/or addition of nucleotides) and ligated to form a coding joint (CJ) on the chromosome; the corresponding SEs are precisely joined to form a signal joint (SJ), which is usually contained on an extrachromosomal circular piece of DNA (for review, see Lewis 1994). SJ formation appears to be much slower than CJ formation, accounting for the fact that only SEs are easily detected in normal developing lymphocytes (Roth et al. 1992; Ramsden and Gellert 1995; Zhu and Roth 1995). Given that RSS cleavage is the initiating event in *V(D)J* recombination, the regulation of recombinational accessibility at specific RSSs can readily be monitored by directly studying these broken-ended DNA intermediates (Constantinescu and Schlissel 1997).

Both transgenic and gene targeting studies demonstrate that immunoglobulin and TCR *cis*-acting regulatory elements, notably transcriptional enhancers, play a critical role in the control of *V(D)J* recombination in vivo (for review, see Sleckman et al. 1996; Hempel et al. 1998). A striking example of the influence of enhancers on gene rearrangement was uncovered through the analysis of engineered mouse mutants carrying a 0.56-kb genomic deletion that removes the only known transcriptional enhancer (Eβ) in the ~500-kb TCRβ locus (Bories et al. 1996; Bouvier et al. 1996). In T cells from both heterozygous ($E\beta^{+/-}$) and homozygous ($E\beta^{-/-}$) Eβ-deleted mice, partial (*D*β-to-*J*β) as well as complete (*V*β-to-*DJ*β) recombination products are dramatically reduced on the targeted allele(s). Consequently, in $E\beta^{-/-}$ mice, development of αβ T cells is selectively impaired (Bouvier et al. 1996), in a manner similar to that in TCRβ-deleted mice (Mombaerts et al. 1992). In this study, we investigated whether the block in TCRβ gene rearrangement observed in the absence of Eβ was caused by altered accessibility of the targeted locus. Our results indicate that, contrary to expectations, the TCRβ enhancer may affect both RSS accessibility as well as a downstream phase of the recombination reaction, thus providing new insights into the mechanism(s) by which enhancers regulate the *V(D)J* recombination process.

Results

SE intermediates of TCRβ gene rearrangement are present in $E\beta^{-/-}$ thymuses

We addressed the issue of RSS accessibility at the targeted TCRβ locus by searching for the presence of broken SE intermediates in $E\beta^{-/-}$ thymuses. Because SEs are 5′ phosphorylated and blunt, they are suitable substrates for ligation-mediated PCR (LM-PCR). This technique has been used extensively to detect the presence of SE intermediates at a number of immunoglobulin and TCR loci in various lymphoid tissues (Schlissel et al. 1993; Roth et al. 1993; Constantinescu and Schlissel 1997). We used LM-PCR to analyze genomic DNA from $E\beta^{-/-}$ thymuses, focusing on the products of recombinase cleavage at *D*β and *J*β gene segments. During normal T cell development, recombination events at the TCRβ locus are ordered such that *D*β-to-*J*β rearrangement occurs first followed by *V*β-to-*DJ*β rearrangement (Born et al. 1985). Therefore, analysis of *D*β and *J*β cleavage reflects the onset of *V(D)J* recombinase activity at this locus. A schematic representation of the LM-PCR strategy used to detect DSBs at RSSs 3′ of *D*β2 and 5′ of *J*β2.1 gene segments is shown in Figure 1A; representative results from these and similar analyses are shown in Figure 1B. Surprisingly, given the fact that *V(D)J* recombination products were not previously found in $E\beta^{-/-}$ thymuses (Bouvier et al. 1996), broken-ended intermediates of rearrangement were readily detected. DSBs were detectable both 5′ and 3′ of the *D*β*2* gene segment in thymus DNA from four individual $E\beta^{-/-}$ mice and DSBs 5′ of the Jβ2.1 gene segment were detectable in DNA from three of the four mice (Fig. 1B, lanes 1,4–6). By use of analogous assays, DSBs have also been found 5′ of the *D*β1 and *J*β1.1 gene segments and 5′ of the *J*β2.5 and *J*β2.6 gene segments (data not shown and see below). Levels of DSBs at the various sites, although variable from mouse to mouse, were consistent within a given sample (for example, the $E\beta^{-/-}$ thymus DNA shown in lane 1 of Fig. 1B had the highest level of DSBs at all TCRβ gene segments analyzed). On average, DSB signals in $E\beta^{-/-}$ thymuses appeared to be lower than those in wild-type and $E\beta^{+/-}$ controls, although this was not a general rule (e.g., see Fig. 1B).

We used several approaches in an attempt to more precisely quantify the difference in steady-state levels of DSBs generated in the absence and presence of Eβ. First, we compared undiluted thymus DNA from several $E\beta^{-/-}$ mice with serial dilutions of thymus DNA from wild-type mice (Fig. 2A). LM-PCR analyses of DSBs 3′ of *D*β2 confirmed interindividual variation in $E\beta^{-/-}$ thymuses and indicated that levels of 3′ *D*β2 SEs are decreased by ~3- to 30-fold in $E\beta^{-/-}$ mice as compared to those in wild-type mice. These estimates were in general agreement with Southern blot analyses in which we compared the hybridization of a *D*β–*J*β region probe to separate digests of kidney (nonrearranging) and thymus DNA and quantified the decrease in hybridization to the thymus sample (data not shown).

Because *D*β-to-*J*β rearrangement normally occurs in TCR^-, $CD4^-$, $CD8^-$ thymocytes (Godfrey et al. 1994), direct comparison of wild-type and $E\beta^{-/-}$ thymocytes might be misleading because of the altered cellular composition of mutant thymus. $E\beta^{-/-}$ thymus consists mostly of low numbers of immature $\alpha\beta TCR^-$, $CD4^-$, $CD8^-$ and mature $\gamma\delta TCR^+$ T cells (Bouvier et al. 1996; I. Leduc, N. Mathieu and P. Ferrier, unpubl.; for average cell numbers and percentages of thymus cells from the various mice used in this study; see Materials and Methods). These cell populations comprise <10% of wild-type thymus. Therefore, we also compared the levels of DSBs

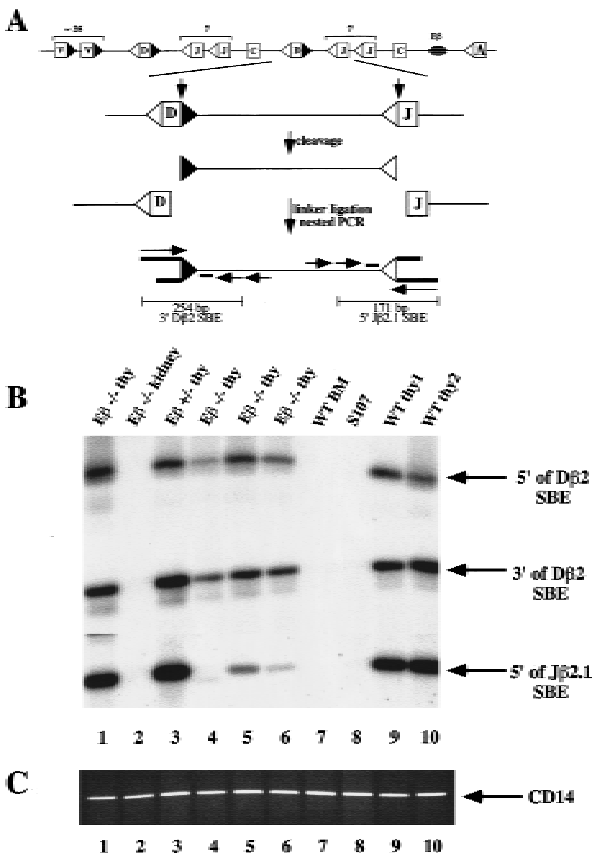

Figure 1. Broken SE intermediates of TCRβ gene rearrangement are present in $E\beta^{-/-}$ thymocytes. (*A*) Schematic diagram of the TCRβ genomic locus (not drawn to scale). *V*, *D*, and *J* gene segments (boxes) are flanked by consensus RSSs containing either 12-bp (open triangles) or 23-bp (closed triangles) spacers. A panel of ~35 *V*β gene segments lies upstream of two clusters of *D*β, *J*β, and *C*β gene segments (Lai et al. 1989; Hood et al. 1995). Each cluster contains a single *D*β segment, seven *J*β segments (one of which is a pseudo-*J*β segment), and a *C*β gene. Recombination is initiated by double-strand cleavage at the junctions between two gene segments and their respective RSSs, as shown for *D*β2-to-*J*β2.1 rearrangement (bold vertical arrows). Broken SE intermediates are detected by ligation of total genomic DNA to a linker (asymmetric pair of bold lines) followed by nested PCR amplification with a linker-specific primer and two locus-specific primers (horizontal arrows). The LM-PCR products are separated on agarose gels, Southern blotted, and hybridized with a third locus-specific oligonucleotide that is end-labeled with [γ-^{32}P]ATP (short bold line). Products of 254-bp and 171-bp are predicted for *D*β2 and *J*β2.1 SEs, respectively. (*B*) Genomic DNA purified from the thymuses of four individual $E\beta^{-/-}$ mice ($E\beta^{-/-}$ thy; lanes *1, 4–6*), an Eβ+/− mouse (lane *3*), and two individual wild-type mice (WT thy1 and WT thy2; lanes *9,10*) was linker-ligated and analyzed by LM-PCR for DSBs at RSSs flanking the *D*β2 and *J*β2.1 gene segments. Linker-ligated DNAs from $E\beta^{-/-}$ kidney (lane *2*), from wild type bone marrow (WT-BM); lane *7*) and a plasmacytoma cell line, S107 (lane *8*), were amplified in parallel as negative controls. (Arrows) broken SEs at the RSS 5′ of *D*β2 (*top*), 3′ of *D*β2 (*middle*) and 5′ of *J*β2.1 (*bottom*). (*C*) Amplification of a control nonrearranging genomic locus, CD14, from the same genomic DNA samples analyzed in *B*.

in *CD3*ϵ-deleted ($\epsilon^{-/-}$; Malissen et al. 1995) thymuses, which are hypocellular and contain only TCR^-, $CD4^-$, $CD8^-$ cells, with those in *TCR*$\delta^{-/-}$ ($\delta^{-/-}$) $E\beta^{-/-}$ double-mutant thymuses, which contain only TCR^-, $CD4^-$, $CD8^-$ cells (Fig. 2B). PCR analyses of 3′ *D*β2 SE levels in $\delta^{-/-}$ $E\beta^{-/-}$ thymuses demonstrated less variation between animals and gave signals that were ~10-fold lower than those in $\epsilon^{-/-}$ mice (Fig. 2B, top panel). Similar analyses of DSBs 5′ of the *J*β2.6 gene segment gave concordant data (Fig. 2B, bottom panel). Quantitative analyses of DSBs at other *J*β2 gene segments revealed somewhat greater decreases in the $E\beta^{-/-}$ thymuses (10- to 100-fold; data not shown). Assuming *D*β-to-*J*β coupled cleavage, the variability in these results could be explained by the structure of the TCRβ locus, which is comprised of two similarly organized clusters each consisting of one *D* and seven *J* segments—one being a pseudo-*J* segment (see Fig. 1A). Within one cluster each *J*β segment is expected to have only a fraction of the level of DSBs as *D*β and not necessarily the same at all *J*βs (e.g., see Candéias et al. 1991).

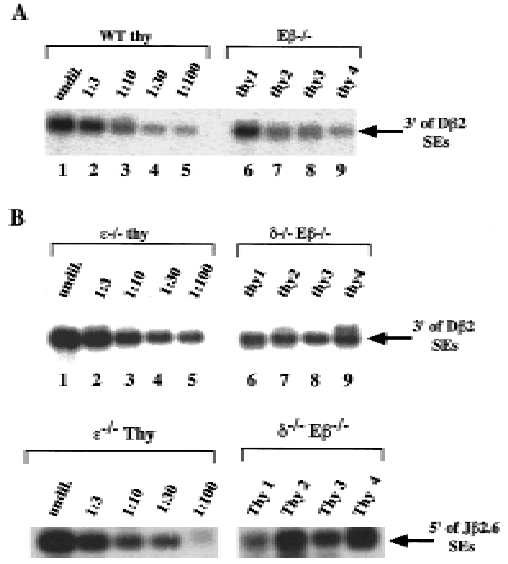

Figure 2. Broken SE intermediates 3′ of *D*β2 and 5′ of *J*β2.6 are only moderately reduced in $E\beta^{-/-}$ versus wild-type and $\delta^{-/-}$ $E\beta^{-/-}$ vs. $\epsilon^{-/-}$ mice. Genomic DNA purified from the thymuses of four individual $E\beta^{-/-}$ mice ($E\beta^{-/-}$ thy1–4), four individual $\delta^{-/-}$ $E\beta^{-/-}$ mice, an $\epsilon^{-/-}$ mouse, and a wild-type mouse (WT mouse 2), and genomic DNA derived from the kidney of an $\delta^{-/-}$ $E\beta^{-/-}$ mouse was linker ligated as diagrammed in Fig. 1A. Linker-ligated wild-type or $\epsilon^{-/-}$ thymus DNA was diluted serially 1 : 3 into linker-ligated $\delta^{-/-}$ $E\beta^{-/-}$ kidney DNA to keep the DNA concentration constant and subjected to LM-PCR with primers specific for the detection of DSBs at the RSS 3′ of *D*β2 (3′ of *D*β2 SEs) or 5′ of *J*β2.6 (5′ of Jβ2.6 SEs), as indicated. Undiluted linker-ligated $E\beta^{-/-}$ or $\delta^{-/-}$ $E\beta^{-/-}$ thymus DNAs were amplified in parallel. $E\beta^{-/-}$ thymus DNAs are the same as those used in the experiments shown in Fig. 1B and C. (*A*) Results of the wild-type thymus DNA titration versus $E\beta^{-/-}$ thymus DNA. (*B*) Results of the $\epsilon^{-/-}$ thymus DNA titrations vs. the $\delta^{-/-}$ $E\beta^{-/-}$ thymus DNA.

TCRβ loci in isolated nuclei from Eβ$^{-/-}$ thymuses are substrates for in vitro cleavage by the V(D)J *recombinase*

The presence of TCRβ DSBs in Eβ$^{-/-}$ thymuses suggests that the recombinase machinery can obtain access to at least some RSSs within the enhancerless TCRβ locus in a significant proportion of developing thymocytes. To confirm this finding, we applied a recently described RAG-mediated in vitro DNA cleavage assay that directly measures the accessibility of RSSs within native chromatin structure. Previous applications of this assay have demonstrated that recombinase access to specific RSSs within various immunoglobulin and TCR loci is a regulated property of lymphocyte chromatin structure (Stanhope-Baker et al. 1996). Thus, susceptibility of TCRβ RSSs to in vitro cleavage in Eβ$^{-/-}$ versus wild-type thymocyte chromatin reflects the importance of Eβ sequences in establishing recombinase accessibility at the TCRβ locus. To perform these analyses, the Eβ deletion was introduced at the homozygous state on a RAG1-deficient (*rag*$^{-/-}$) background (so that there are no preexisting RSS breaks at any immunoglobin or TCR locus). Thymocyte nuclei isolated from the *rag*$^{-/-}$ Eβ$^{-/-}$ double mutants and from *rag*$^{-/-}$ controls were incubated with purified recombinant core RAG1 protein (rRAG1) and cow thymus nuclear extract, as described previously (Stanhope-Baker et al. 1996). Generation of DSBs in vitro, indicative of recombinase access to specific RSSs, was monitored by LM–PCR. Figure 3 shows the results from an experiment analyzing in vitro cleavage at RSSs 3′ of *D*β2 and, as a control, 5′ of the immunoglobulin–*J*κ5 segment (the Igκ locus is not rearranged in T lineage cells). In vitro-generated *D*β2 DSBs, but not *J*κ5 DSBs, were detected in reactions containing either *rag*$^{-/-}$ or *rag*$^{-/-}$ Eβ$^{-/-}$ nuclei (lanes 1–6). Conversely, in vitro reactions containing purified genomic DNA from *rag*$^{-/-}$ or *rag*$^{-/-}$ Eβ$^{-/-}$ thymuses showed de novo cleavage of both *D*β2 and *J*κ5 RSSs (lanes 7–10). *D*β2 DSBs and, as shown previously, *J*κ5 DSBs generated in vivo can be detected in genomic DNA from wild-type thymus or from wild-type bone marrow and spleen, respectively (lanes 11–13), and none is found in *rag*$^{-/-}$ or *rag*$^{-/-}$ Eβ$^{-/-}$ thymuses (lanes 14,15) (Schlissel et al. 1993; Constantinescu and Schlissel 1997). In separate experiments, identical results were obtained by use of purified nuclei from a different *rag*$^{-/-}$ Eβ$^{-/-}$ mouse (data not shown). In vitro cleavage 3′ of *D*β2 was also observed in reactions containing nuclei from a pro-B cell line but not in those containing nuclei from fibroblasts (data not shown), indicating that recombinase targeting of this site is regulated, at least in part, by its accessibility within chromatin. Finally, with the same *rag*$^{-/-}$ and *rag*$^{-/-}$ Eβ$^{-/-}$ nuclei samples, in vitro cleavage 5′ of both *Dβ2* and *Jβ2.1* gene segments was also observed (data not shown). Although we did not attempt to quantitate the relative levels of DSBs generated in vitro in *rag*$^{-/-}$ versus *rag*$^{-/-}$ Eβ$^{-/-}$ thymocyte nuclei, they were roughly equivalent in several separate experiments (Fig. 3, cf. lanes 2 and 3 to lanes 5 and 6, and data not shown). Our observation that *J*κ5 DSBs were not detected in reactions containing either *rag*$^{-/-}$ or *rag*$^{-/-}$ Eβ$^{-/-}$ nuclei strongly suggests that *V(D)J* recombinase components (e.g., RAG factors) were not used at saturating levels in these assays. Also, under these in vitro conditions, SJ formation was not detected (P. Stanhope-Baker and M. Schlissel, unpubl.). Taken together, these results suggest that Eβ has at most a modest effect on TCRβ locus accessibility as measured by this assay. The larger difference we observed in in vivo-generated DSBs between wild-type and Eβ$^{-/-}$ thymuses (described above) could reflect, in the mutant thymocytes, either a decrease in the amount of DSBs generated in vivo or a decrease in their life span attributable, for example, to increased apoptosis of cells with unresolved DSBs (see below).

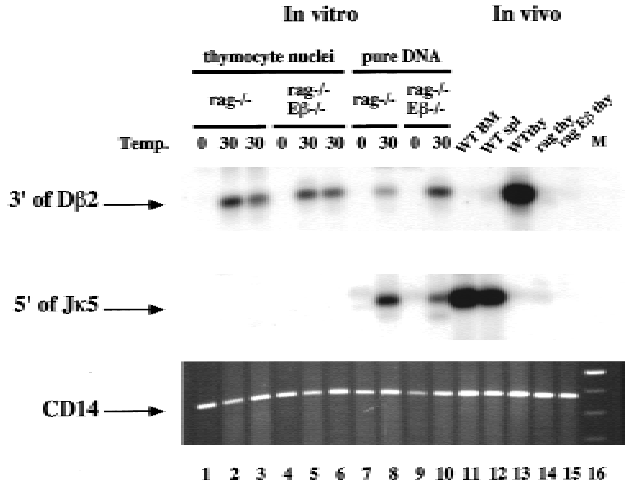

Figure 3. The TCRβ locus is accessible to in vitro cleavage by the *V(D)J* recombinase in Eβ$^{-/-}$ thymocyte nuclei. Intact nuclei (lanes 1–6) or purified genomic DNA (lanes 7–10) from rag$^{-/-}$ or rag$^{-/-}$ Eβ$^{-/-}$ thymocytes were incubated with fetal cow thymus nuclear extract and rRAG1 protein at 30°C (30) or on ice (0) for 60 min. DNA recovered from the reactions was linker-ligated and assayed for in vitro cleavage within the TCRβ locus (3′ of *D*β2, *top*) and the Igκ light chain locus (5′ of Jκ5, *middle*). Broken SE intermediates at each site were amplified by LM-PCR essentially as described in Fig. 1A, the only difference being the locus-specific primers and probes used. Breaks generated in vivo in wild-type bone marrow (WTBM; lane *11*), spleen (WT spl; lane *12*) and thymus (WTthy; lane *13*) as well as rag$^{-/-}$ thymus (lane *14*) and rag$^{-/-}$ Eβ$^{-/-}$ thymus (lane *15*) were amplified in parallel. (Bottom) Amplification of a control nonrearranging gene (CD14) from each sample, confirming that similar amounts of DNA were recovered from all in vitro cleavage reactions.

Differences in steady-state levels of D*β-to-*J*β CJs and SJs in Eβ$^{-/-}$ thymocytes*

Our finding that a significant proportion of *D*β and *J*β gene segments in Eβ$^{-/-}$ thymocytes remains accessible to recombinase cleavage both in vivo and in vitro raises the question of why *D*β-to-*J*β CJs were not readily found in thymus DNA from *Eβ*$^{-/-}$ mice with conventional PCR assays (Bouvier et al. 1996, and data not shown). One possibility is that, in the absence of Eβ, there is a

defect in the late phase of the *V(D)J* recombination reaction that specifically affects broken end processing and/or joining. Alternatively, broken-ended intermediates could be processed correctly but directed toward alternative *V(D)J* junctions. To explore the role of Eβ in directing recombination further, we searched for the presence of standard TCRβ CJs and SJs as well as nonstandard products of *V(D)J* recombination (see below) in Eβ$^{-/-}$ thymocytes, by use of sensitive nested PCR assays. We found that *D*β-to-*J*β CJs involving several *J*β2 genes could be detected in thymus DNA from most Eβ$^{-/-}$ mice that we analyzed, including the four Eβ$^{-/-}$ DNAs previously shown to contain *D*β and *J*β SEs (Fig. 4; data not shown). However, the relative level of CJs found in the Eβ$^{-/-}$ samples was extremely low (a reduction of at least 100-fold) as compared to wild-type controls (e.g., see Fig. 4, lanes 6–9); similar analysis of δ$^{-/-}$ Eβ$^{-/-}$ thymus DNAs gave concordant results (data not shown). These numbers most likely represent overestimations of CJ frequency in the mutant mice as wild-type *DJ*β alleles, but not enhancerless *DJ*β alleles, undergo *V*β-to-*DJ*β recombination (Bories et al. 1996; Bouvier et al. 1996; W. Hempel, N. Mathieu, and P. Ferrier, unpubl.) and thus become invisible to the *DJ*β coding joint assay. Sequence analysis of the rare CJs formed in an Eβ$^{-/-}$ thymus showed the hallmarks of normal CE processing prior to joint formation (Fig. 5A). We conclude that although *D*β-to-*J*β CJs are formed very inefficiently in Eβ$^{-/-}$ thymocytes, they appear to be the products of normal *V(D)J* joining reactions.

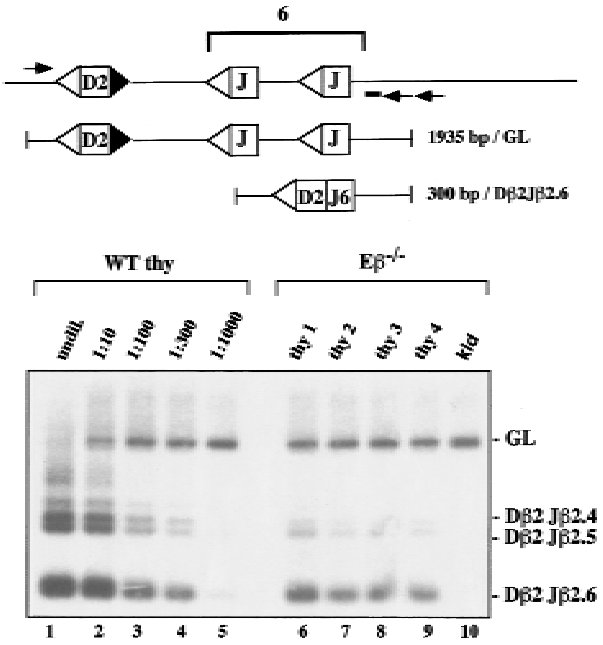

Figure 4. *D*β2-to-*J*β2 CJ formation is dramatically reduced in Eβ$^{-/-}$ thymus DNA. A nested PCR reaction was used to detect *D*β2–*J*β2 coding joints. PCR primers (horizontal arrows) 5′ of *D*β2 and 3′ of *J*β2.6 allow detection of CJs involving *D*β2 and either *J*β2.4, *J*β2.5, or *J*β2.6 (*D*β2 rearrangements to other *J*β2 gene segments result in PCR products too large to efficiently amplify under these conditions). PCR products were blotted and hybridized with a specific probe (short bold line). The structure and sizes of amplified germ-line and rearranged products are shown schematically. Genomic DNA purified from wild-type mouse thymus (WT mouse #2) was serially diluted 1 : 10, 1 : 100, 1 : 300 and 1 : 1000 into kidney DNA derived from a δ$^{-/-}$ Eβ$^{-/-}$ mouse to keep the DNA concentration constant. The diluted wild-type thymus DNA (lanes *1–5*), undiluted thymus DNA from four Eβ$^{-/-}$ mice (lanes *6–9;* Eβ$^{-/-}$ mice #1 to #4, corresponding to DNA samples shown in Figs. 1 and 2), Eβ$^{-/-}$ kidney DNA (lane *9*) and Eβ+/− thymus DNA (lane *10*) were amplified by use of the nested PCR scheme shown at the *top* of the figure. The identities of the amplified products are indicated at the *right* of the gel.

Given our finding of relatively high levels of SEs in Eβ$^{-/-}$ thymocytes, we searched for SJs involving extrachromosomal joining of *D*β2 and *J*β2 SEs using appropriate PCR assays (Fig. 6, legend). To confirm the structure of the putative SJs, the amplified products were digested with the restriction endonuclease *Apa*LI, which recognizes a site generated by precise RSS joining. Significantly, we could detect SJs resulting from the fusion of RSSs 3′ of *D*β2 and 5′ of several *J*β2 segments in the four Eβ$^{-/-}$ thymus DNAs analyzed throughout this study, implying that *D*β-to-*J*β coupled cleavage most likely occurs in the absence of Eβ and that at least some of the resulting SEs are competent for joining. Figure 6 shows representative data for SJs involving the *D*β2 and *J*β2.6 RSSs (Fig. 6A) and attempts to quantify these products (Fig. 6B). Levels of *D*β2-to-*J*β2.6 SJs appear to be reduced by ~5- to 25-fold in Eβ$^{-/-}$ thymuses as compared to wild-type controls. It might be argued that the intense cell proliferation which, in wild-type thymuses, gives rise to large numbers of CD4$^+$ CD8$^+$ double positive (DP) thymocytes would tend to dilute extrachromosomal SJ products (e.g., see Livak and Schatz 1996), leading to an overestimation of SJs in Eβ$^{-/-}$ thymuses. In a separate experiment, where Dβ2-to-Jβ2 SJs were analyzed using δ$^{-/-}$ Eβ$^{-/-}$ and ε$^{-/-}$ DNAs (to restrict our analysis to TCR$^-$, CD4$^-$, CD8$^-$ thymocytes), we found that SJs were ~100-fold lower in δ$^{-/-}$ Eβ$^{-/-}$ versus ε$^{-/-}$ thymuses (data not shown). In any case, when compared within each individual Eβ$^{-/-}$ thymus DNA sample, the relative levels of *D*β2-to-*J*β2 SJs always appear to be higher than that of the corresponding CJs, strongly suggesting that the Eβ deletion affects coding joint formation more drastically.

Nonstandard V(D)J *rearrangements within enhancerless TCRβ alleles*

Finally, we have analyzed Eβ$^{-/-}$ and wild-type thymus DNAs for the presence of several nonstandard products of *V(D)J* recombination that involve *D*β and/or *J*β broken-ended intermediates. One such product, called a hybrid joint (HJ), results from the fusion of a CE to the SE from the recombination partner. HJs are formed at low but detectable levels in wild-type mice (Lewis 1994), as well as in Ku86 knockout (*Ku86*$^{-/-}$) and *scid* mice, which are both defective in CJ formation (as well as in SJ formation in the case of the *Ku86*$^{-/-}$ mice) (Zhu et al. 1996; Nussenzweig et al. 1996; Bogue et al. 1997). Although we readily detected HJs between *D*β2 and *J*β2

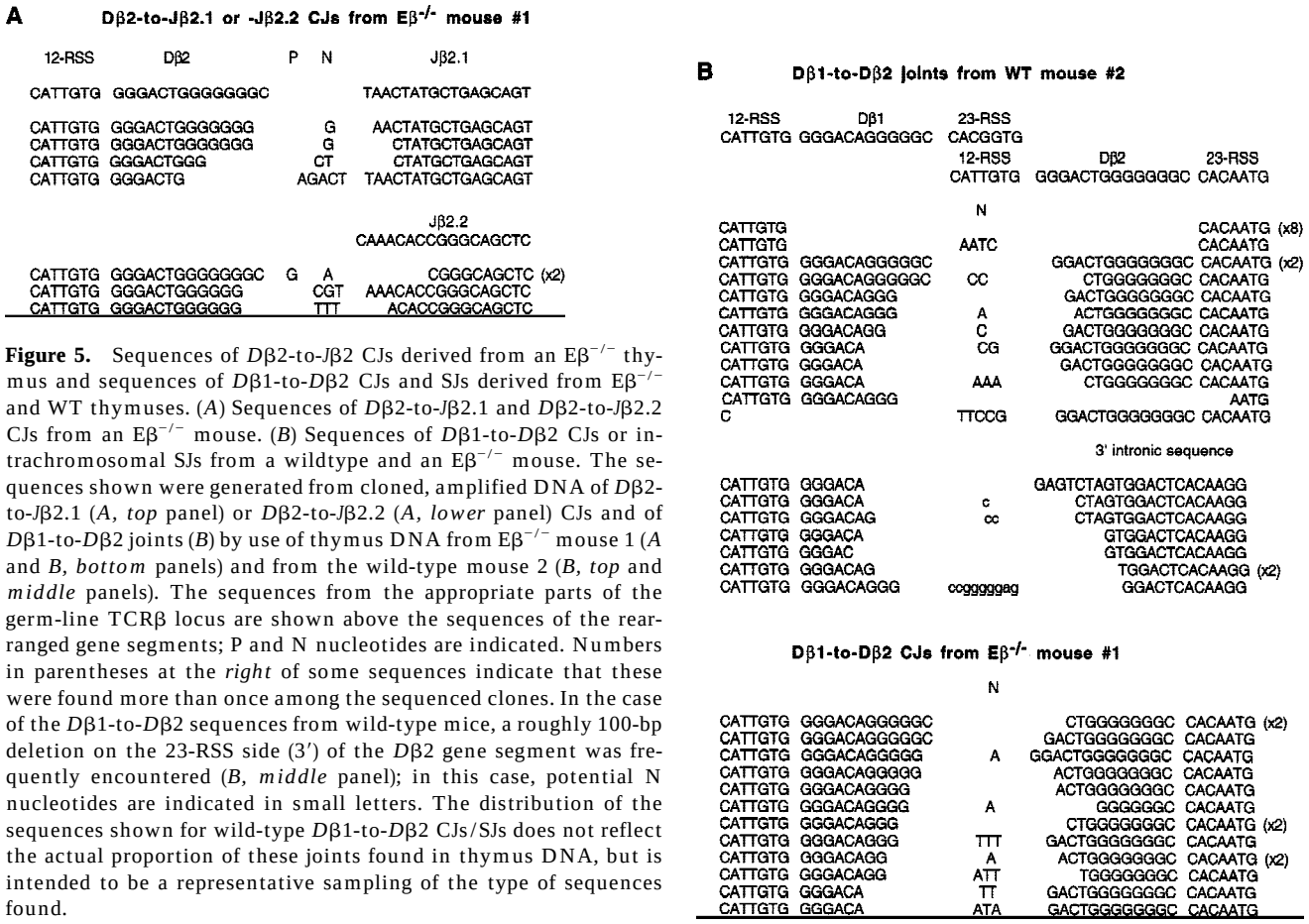

Figure 5. Sequences of *D*β2-to-*J*β2 CJs derived from an Eβ$^{-/-}$ thymus and sequences of *D*β1-to-*D*β2 CJs and SJs derived from Eβ$^{-/-}$ and WT thymuses. (*A*) Sequences of *D*β2-to-*J*β2.1 and *D*β2-to-*J*β2.2 CJs from an Eβ$^{-/-}$ mouse. (*B*) Sequences of *D*β1-to-*D*β2 CJs or intrachromosomal SJs from a wildtype and an Eβ$^{-/-}$ mouse. The sequences shown were generated from cloned, amplified DNA of *D*β2-to-*J*β2.1 (*A, top* panel) or *D*β2-to-*J*β2.2 (*A, lower* panel) CJs and of *D*β1-to-*D*β2 joints (*B*) by use of thymus DNA from Eβ$^{-/-}$ mouse 1 (*A* and *B, bottom* panels) and from the wild-type mouse 2 (*B, top* and *middle* panels). The sequences from the appropriate parts of the germ-line TCRβ locus are shown above the sequences of the rearranged gene segments; P and N nucleotides are indicated. Numbers in parentheses at the *right* of some sequences indicate that these were found more than once among the sequenced clones. In the case of the *D*β1-to-*D*β2 sequences from wild-type mice, a roughly 100-bp deletion on the 23-RSS side (3′) of the *D*β2 gene segment was frequently encountered (*B, middle* panel); in this case, potential N nucleotides are indicated in small letters. The distribution of the sequences shown for wild-type *D*β1-to-*D*β2 CJs/SJs does not reflect the actual proportion of these joints found in thymus DNA, but is intended to be a representative sampling of the type of sequences found.

segments in wild-type, *Ku86*$^{-/-}$, and *scid* thymuses, we could not detect them in Eβ$^{-/-}$ thymuses (data not shown). These results indicate that this type of nonstandard junction does not contribute significantly to the recombination potential of alleles lacking Eβ. The structural organization of the TCRβ locus, comprised of two clusters of *D*β and *J*β gene segments (Lai et al. 1989; Hood et al. 1995), permits formation of a second type of nonstandard junction. Recombination can occur between *D*β gene segments in the two TCRβ clusters resulting in *D*β1-to-*D*β2 joints. Using a PCR assay, we found *D*β1-to-*D*β2 products in thymus DNA from wild-type mice as well as in thymus DNA from all four Eβ$^{-/-}$ mice (Fig. 7). Interestingly, while some of the amplified products from wild-type thymuses were digested with *Apa*LI, suggesting that they are comprised of at least some intrachromosomal SJs, those from the Eβ$^{-/-}$ thymuses were not. These joints are therefore likely to represent *D*β1-to-*D*β2 CJs or imprecise SJs. These hypotheses were verified by cloning and sequencing the PCR products (see Fig. 5B). Strikingly, while intrachromosomal *D*β1-to-*D*β2 SJs represented ~1/3 of the PCR products sequenced from a wild-type thymus, none were found among those from an Eβ$^{-/-}$ thymus (Fig. 5B, cf. upper and lower panels). Joints amplified from an Eβ$^{-/-}$ thymus included exclusively *D*β1-to-*D*β2 CJs, which appeared to be the products of normal *V(D)J* joining reactions. This was also the case for some of the CJ products amplified from a wild-type thymus (top panel). However, the later products also frequently showed aberrant structural features, most of them involving deletion of *D*β2 downstream sequences including the 3′ *D*β2 RSS (top panel and middle panel).

Discussion

Gene targeting analyses have confirmed that transcriptional enhancers play an important role in the *cis*-regulation of immunoglobulin and TCR genes during *V(D)J* recombination (for review, see Sleckman et al. 1996; Hempel et al. 1998). In each case, it has been postulated that the observed phenotype is a result of reduced recombinational accessibility, but this has not been formally demonstrated. In this study, we evaluated the consequences of enhancer deletion on the various steps of the *V(D)J* recombination reaction at an endogenous TCR gene locus. Using Eβ$^{-/-}$ mice as a model, we unexpectedly found that the *V(D)J* recombinase can still obtain access to, and be active at, the mutated TCRβ alleles. Specifically, our observation that RSSs flanking *D*β and *J*β gene segments are readily cleaved by the *V(D)J* recombinase in Eβ$^{-/-}$ thymocytes, both in vivo and in vitro, implies that control of *D*β-to-*J*β rearrangement by the TCRβ enhancer is not attributable solely to modulation

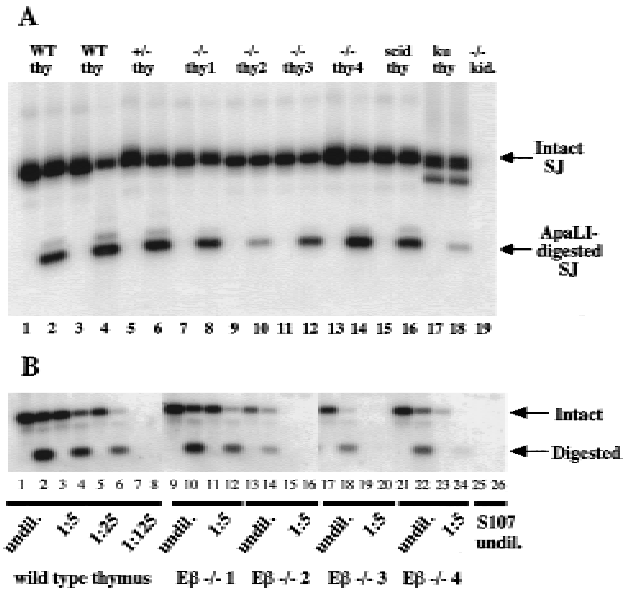

Figure 6. Broken TCRβ SEs are resolved into SJs in Eβ$^{-/-}$ thymocytes. SJ formation involving a 3′ of Dβ RSS and a 5′ of Jβ RSS results in an extrachromosomal circular product of characteristic structure. Each broken SE generated by recombinase cleavage is blunt and shows no loss or gain of nucleotides from the conserved RSS. Therefore, fusion of these ends generates a new site for the enzyme *Apa*LI (5′-GTGCAC-3′). Dβ-to-Jβ SJs of this structure can be detected in a pool of total genomic DNA by PCR amplification with primers on either side of the junction and hybridization with an internal oligonucleotide probe. Precision of amplified signal joints can be confirmed by *Apa*LI digestion. Digestion will result in two products of defined size, one of which will hybridize to the probe. (*A*) SJs involving *D*β2 and *J*β2.6 RSSs were amplified from genomic DNA by use of a scheme similar to that described above, except that nested primers were used in a two-step PCR reaction. Following amplification, one-half of each PCR product was digested with *Apa*LI at 37°C (even numbered lanes) and the other half was mock digested with a heat-inactivated irrelevant restriction enzyme on ice (odd numbered lanes). The reaction products were then resolved on an agarose gel, Southern blotted, and hybridized with an oligonucleotide probe that will detect the undigested SJ (intact SJ) as well as one of the two fragments generated by *Apa*LI cleavage of the SJ (*Apa*LI-digested SJ). Reactions contained template genomic DNA from two independent wild-type thymuses (lanes 1-4), an Eβ+/− thymus (lanes *5, 6*), four individual Eβ$^{-/-}$ thymuses (lanes *7–14*), a scid thymus (lanes *15,16*), a Ku86$^{-/-}$ thymus (lanes *17, 18*) or Eβ$^{-/-}$ kidney (lane *19*). (*B*) Quantitation of *D*β-to-*J*β SJs. Serial five-fold dilutions of genomic DNA from a wild-type thymus and four independent Eβ$^{-/-}$ thymuses were made into genomic DNA from the S107 plasmacytoma cell line. Extrachromosomal SJs involving the *D*β2 and *J*β2.6 RSSs were amplified from each sample using a two-step nested PCR reaction exactly as in *A*. One-half of each PCR product was digested with *Apa*LI (even numbered lanes) and the other half was mock digested (odd numbered lanes). The source of DNA and its dilution factor are indicated below each pair of lanes. The intact and digested products of the expected sizes are indicated by arrows. S107 cells do not rearrange TCRβ genes and therefore do not contain detectable TCRβ signal joints (lanes *25,26*).

of RSS accessibility. Furthermore, unanticipated differences in the efficiency with which TCRβ recombination products are generated in Eβ$^{-/-}$ thymocytes strongly suggest a novel function(s) of Eβ in the later (e.g., joining) phase of the *V(D)J* recombination reaction. These results have important implications for our understanding of the role of enhancer sequences in the initiation and/or completion of the *V(D)J* rearrangement process.

Do LM-PCR assays of DSBs accurately reflect the accessibility of the TCRβ locus?

LM-PCR measures the steady-state level of free SEs that exist in a cell population. This level is determined not only by the amount of cleavage but also by the tendency for the SEs to be processed into a form unavailable for LM-PCR. In this regard, three observations are worth mentioning. First, we readily found SJs resulting from the fusion of RSSs 3′ of *D*β and 5′ of *J*β gene segments in thymus DNA from Eβ$^{-/-}$ mice (Fig. 6), implying that, in the absence of Eβ, SEs are competent for joining. Hence, signal joint formation interferes with our ability to de-

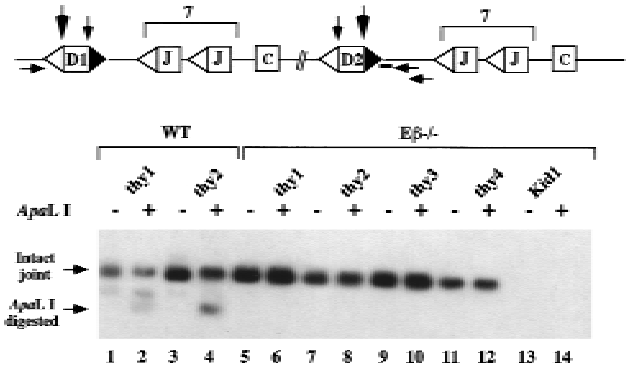

Figure 7. *D*β1-to-*D*β2 joints in wild-type and Eβ$^{-/-}$ thymus DNAs. Genomic DNA from the thymuses of two individual wild-type mice (WT mouse 1 and 2; lanes *1–4*) and four individual Eβ$^{-/-}$ mice (Eβ$^{-/-}$ mouse 1 to 4; lanes *5–12*) was subjected to nested PCR with primers specific for the detection of potential CJs and/or SJs between the *D*β1 and *D*β2 gene segments. DNA from Eβ$^{-/-}$ kidney (lanes *13, 14*) was included as a negative control. Following amplification, one-half of each PCR product was digested with *Apa*LI at 37°C (+) and the other half was mock digested with a heat-inactivated irrelevant restriction enzyme on ice (−), to test for the presence of precise SJs. A schematic diagram of the rearranging gene segments and nested PCR assay is shown at the *top* of the figure. The positions of the PCR primers are indicated by horizontal arrows and the probe is shown as a horizontal bar. Recombination between *D*β1 and *D*β2 is initiated by recombinase cleavage at the junction between each coding segment and its flanking RSS (vertical arrows). Coupled cleavage according to the 12/23 rule can occur in two ways at these sites (large and small vertical arrows). Coupled cleavage at the sites indicated by the large pair of arrows leads to intrachromosomal *D*β1-to-*D*β2 SJ formation. Cleavages indicated by the small pair of arrows leads to *D*β1-to-*D*β2 CJ formation. The sizes of the SJ and CJ products differ only by the length of the *D*β segments (25 bp) and are not distinguishable on this gel.

tect SEs in both wild-type and mutant TCRβ loci. Second, we found no evidence that nonpairwise (e.g., uncoupled) cleavage is increased in the Eβ$^{-/-}$ thymocytes. Because singly cleaved *D*β or *J*β segments would result in SEs available for LM-PCR but unable to form SJs, such an effect would potentially lead to an underestimation of the difference in cleavage between the Eβ$^{-/-}$ and wild-type TCRβ loci. We tested mutant DNA for singly cleaved *J*β2 segments by using primers 5′ of the *D*β2 gene segment to perform an LM-PCR analysis of RSS breaks 5′ of *J*β2 gene segments (data not shown). This approach failed to reveal *J*β2 DSBs; instead, mutant and wild-type DNAs exhibited a fragment ending at the RSS 5′ of the *D*β2 segment (e.g., 5′ *D*β2 SEs), as expected. Third, the level of DSBs 3′ of the *D*β2 gene segment (as measured by LM-PCR) is lower in thymus from Ku86-deficient mice (*Ku86*$^{-/-}$) than in thymus from wild-type, $\epsilon^{-/-}$, $\delta^{-/-}$ Eβ$^{-/-}$ and Eβ$^{-/-}$ mice (W. Hempel, unpubl.). *Ku86*$^{-/-}$ mice undergo *V(D)J* cleavage but are defective in both SJ and CJ formation (Zhu et al. 1996; Nussenzweig et al. 1996; Bogue et al. 1997). We suspect that the decreased frequency of DSBs in *Ku86* mutant thymocytes is because these thymocytes frequently undergo apoptosis because of unresolved DSBs. Because *D*β-to-*J*β joining is also impaired in the absence of Eβ (Fig. 4), it is possible that Eβ mutant thymocytes might also frequently undergo apoptosis, leading us to underestimate the frequency of DSBs. Our observation of apparently equivalent accessibility of TCRβ RSSs in nuclei purified from *rag*$^{-/-}$ and *rag*$^{-/-}$ Eβ$^{-/-}$ mice is consistent with this notion (see Fig. 3).

The TCRβ enhancer and the control of RSS accessibility

We emphasize that the extent to which RSS accessibility within the *D*β–*J*β clusters may be independent of Eβ (as well as the relative impact of Eβ on *D*β vs. *J*β accessibility—discussed further below) is unclear at the moment. Our in vivo analyses would indicate that deletion of the Eβ element results in a ~10-fold loss of *V(D)J* recombinase activity at the *D*β2–*J*β2 locus as measured by SE formation (see Fig. 2B). As noted above, these analyses may underestimate the relative levels of RSS breaks produced at mutant alleles, and in vitro RSS cleavage assays suggested roughly equivalent levels of DSBs at the *D*β2 gene segment in Eβ$^{+/+}$ and Eβ$^{-/-}$ nuclei. However, because RSSs 3′ of *D*β2 were found to be cleaved in vitro in nuclei from lymphoid cells but not fibroblasts (Fig. 3, and data not shown), recombination of the TCRβ locus must be regulated, at least in part, by its accessibility within chromatin. Therefore, the surprisingly moderate decrease in RSS cleavage that was observed in the Eβ$^{-/-}$ thymuses raises the possibility that, besides Eβ, another element exists in the TCRβ locus that is responsible for controlling accessibility. Alt and colleagues came to the same conclusion, based on the T-cell restricted activity of the *V(D)J* recombinase at the TCRβ locus in mice carrying the immunoglobulin heavy (H) chain intronic enhancer in place of the Eβ element (Bories et al. 1996). Ongoing analyses on the chromatin structure of *D*β and *J*β sequences in the Eβ$^{-/-}$ mice may help to clarify these issues (N. Mathieu, W. Hempel and P. Ferrier, in prep.).

Because *V(D)J* recombination involves coupled cleavage of pairs of gene segments, regulation of recombination by enhancers could in principle be exerted through the tight control of accessibility of a limited array of gene segments. Such a local effect has recently been proposed in the case of the TCRδ enhancer, on the basis of the observation that, in human TCRδ transgenic miniloci, RSS cleavage at the *J*δ1 segment, but not at the *D*δ3 segment ~1.0 kb upstream, was enhancer dependent (McMurry et al. 1997). The unusual prevalence of *D*β-to-*D*β CJs in Eβ$^{-/-}$ thymocytes may be viewed as evidence that, similarly, accessibility of *J*β segments is dependent on Eβ function, whereas that of *D*β segments is not. However, several lines of reasoning lead us to believe that this is not the case. First, the fact that *J*β SEs and *D*β2-to-*J*β2 SJs can readily be detected in Eβ$^{-/-}$ thymuses strongly argues for *D*β-to-*J*β coupled cleavage in the absence of Eβ. Second, because no intrachromosomal SJs were found following *D*β1-to-*D*β2 recombination in Eβ$^{-/-}$ thymocytes (see Figs. 5 and 7) and given the inherent preference of the RAGs for pairwise 12/23 bp RSS cleavage (Steen et al. 1996, 1997), this type of nonstandard rearrangement cannot de facto account for the SEs 3′ of *D*β2 detected in vivo. Finally, the quantitative and/or qualitative differences in various joints between Eβ$^{-/-}$ and wild-type thymocytes may indicate that *D*β-to-*J*β and *D*β-to-*D*β rearrangements are differentially dependent on Eβ for joining rather than for RSS accessibility (also see below). Thus, enhancer control of *D*-to-*J* recombination may differ in the TCRβ and TCRδ loci. This would account, at least in part, for the facts that *D*-to-*D* junctions are frequent at the wild-type TCRδ but not TCRβ locus and that unlike TCRβ, *V*-to-*D* precedes *VD*-to-*J* recombination at the TCRδ locus (Chien et al. 1987; Lauzurica and Krangel 1994). Confirmation of these assumptions awaits the production and analysis of TCRδ enhancer knockout mice. More generally, analysis of *V(D)J* recombination intermediates and final products in lymphoid cells from the various available immunogobulin and TCR enhancer targeted mice should shed light on the relative influence of each enhancer on RSS accessibility versus the later steps of the recombination reaction. In this respect, our current finding that Eβ lacks an exclusive role in promoting *V(D)J* recombinational accessibility may well parallel previous studies showing that the IgH intronic enhancer as well as the Igκ intronic and 3′ enhancers were all shown to be partly dispensable for recombination at their respective loci (Serwe and Sablitzky 1993; Chen et al. 1993; Xu et al. 1996; Gorman et al. 1996; for review, see Sleckman et al. 1996; Hempel et al. 1998).

The TCRβ enhancer and the control of V(D)J *joining*

How might transcriptional enhancers regulate gene rearrangement in a way other than RSS accessibility? The findings that TCRβ accessibility is moderately affected

in the Eβ$^{-/-}$ thymocytes while *D*β-to-*J*β CJs are severely reduced suggest a specific role for Eβ in *D*β-to-*J*β CJ formation. The lesser reduction in SJ formation suggests a less critical role for Eβ in that joining event. Given the link between transcription and DNA repair (Friedberg 1996), it is possible that Eβ might serve to recruit DNA repair factors to the recombinase. Differences between the mechanisms of joint formation might result in recruited factors being more important for CJ formation than SJ formation. Differential metabolism of CEs and SEs is a hallmark of the *V(D)J* recombination reaction (for review, see Lewis 1994; Gellert 1997). SJ formation, known from independent studies to be less dependent on DNA repair factors (Lieber et al. 1988; Errami et al. 1996), might be less dependent on this enhancer activity. Alternatively, the differential effect of Eβ on the formation of CJs versus SJs may reflect the effects of Eβ-bound proteins on the stability of post-cleavage CE and SE DNA–protein complexes. Recent data from several labs using various in vitro *V(D)J* recombination assays have revealed the existence of such complexes (Agrawal and Schatz 1997; Leu et al. 1997; Ramsden et al. 1997; Weis-Garcia et al. 1997). Enhancer-associated factors could, for example, be required to maintain CEs within a post-cleavage synaptic complex necessary for efficient CJ formation.

Our current results do not provide any clues to the type of factors or the molecular mechanism(s) that may be involved in mediating Eβ's effect on *V(D)J* recombination. The predominant reduction in CJs seen during *D*β-to-*J*β recombination in Eβ$^{-/-}$ mice is reminiscent of the more general *scid* defect in the mouse, which has recently been linked to a nonsense mutation in the kinase domain of DNA-dependent protein kinase (DNA-PK; Blunt et al. 1996; Danska et al. 1996). However, complete failure to recruit DNA-PK activity is unlikely to account for the *V(D)J* recombination defect in Eβ$^{-/-}$ mice since sequence analysis of rare TCRβ CJs from these mice did not reveal the features characteristic of *scid* CJs (Weaver 1995; Lieber et al. 1997). In addition, in contrast to *scid* mice (Weaver 1995; Lieber et al. 1997; Danska et al. 1994), *D*β-to-*J*β HJs were not increased in Eβ$^{-/-}$ thymocytes; likewise, γ-irradiation of newborn Eβ$^{-/-}$ mice did not increase *D*β-to-*J*β CJ formation as it does in scid mice (N. Mathieu and P. Ferrier, unpubl.).

While the profound decrease in *D*β-to-*J*β CJs and HJs in Eβ$^{-/-}$ thymocytes suggests that the corresponding CEs are incompetent for joining in the absence of Eβ, the presence of *D*β-to-*D*β CJs might argue against a general role of enhancer sequences in the joining phase of the *V(D)J* recombination reaction. *D*β-to-*D*β joining may not correspond to typical *V(D)J* recombination events, however. For example, no definitive evidence of *D*β1-to-*D*β2 joints could be found in an examination of >600 sequences representing TCRβ transcripts in various purified T cell populations (Candéias et al. 1991; S. Candéias, pers. comm.). Moreover, our PCR and sequence analyses indicate that *D*β-to-*D*β rearrangements in wild-type and Eβ$^{-/-}$ thymocytes are qualitatively different. The rare *D*β-to-*D*β joints detected in wild-type thymocytes include a large proportion of intrachromosomal SJs and aberrant CJs. Neither of these classes of joints were detected in Eβ$^{-/-}$ mice (Figs. 5B and 7). Finally, preliminary LM-PCR analyses of Eβ$^{-/-}$ thymocytes have revealed low levels of DSBs at RSSs flanking some *V*β gene segments, whereas CJs involving *V*β-to-*DJ*β or *V*β-to-*D*β segments have not been detected. These observations confirm the inability of *D*β segments from Eβ$^{-/-}$ mice to form proper CJs (Bouvier et al. 1996; W. Hempel and P. Ferrier, unpubl.). We suggest that *D*β1-to-*D*β2 joints in the Eβ$^{-/-}$ mice represent highly selected events that may be required to maintain chromosomal integrity and allow survival of the mutant thymocytes. We further suggest that, taken together, our results raise the provocative possibility that Eβ normally targets the recombinase machinery to perform preferentially certain types of TCRβ rearrangements, such as *D*β-to-*J*β, in a manner relatively independent of regulated RSS accessibility.

Although the precise mechanism of how this selective targeting might be achieved is not yet clear, it may involve long-range interactions between enhancers and other *cis*-regulatory elements exerting a local effect. Regulatory sequences endowed with an activating yet localized effect on *V(D)J* recombination, which are believed to contain a promoter active in germ-line transcription, have recently been identified by gene targeting upstream of the TCR-*J*α gene cluster (Villey et al. 1996). Other types of relevant *cis*-acting sequences might include enhancer-blocking (also called boundary) elements (Zhong and Krangel 1997). In the event that such elements exist in the TCRβ locus, our experiments suggest that they may be located in the vicinity of the *J*β1 and *J*β2 gene clusters (i.e., at ~20.2 and ~11.3 kb upstream of Eβ, respectively). The characterization of these potential regulatory elements may be critical for the complete understanding of how the specific utilization of rearranging gene segments is controlled at the TCRβ locus.

Materials and methods

Mice

All mice used in this study, including wild-type C57BL/6J mice, single knockout CD3ϵ deficient (ϵ$^{-/-}$) (Malissen et al. 1995), RAG1-deficient (*rag*$^{-/-}$) (Spanopoulou et al. 1994), heterozygous (Eβ$^{+/-}$) and homozygous (Eβ$^{-/-}$) Eβ-deleted (Bouvier et al. 1996) mice and double knock-out TCRδ-deficient (δ$^{-/-}$) Eβ$^{-/-}$ or RAG1-deficient (*rag*$^{-/-}$) Eβ$^{-/-}$ mice (see below), were maintained in a specific pathogen-free (SPF) breeding facility and were sacrificed for analysis between 4 and 6 weeks of age. Knockout mouse lines were bred on a C57BL/6J genetic background for at least eight successive generations. Thymuses from 4-week-old wild-type (C57BL/6J) or Eβ$^{+/-}$ mice contain $250 \pm 50 \times 10^6$ thymocytes on average, which are comprised of ⩽8% double negative (DN), ⩾80% DP and ~10% TCRαβ$^+$, CD4$^+$, or CD8$^+$ single positive (SP) cells; usually, TCRγδ$^+$ thymocytes do not exceed 2%–3% and are found among the DN cell subpopulation; typically, thymocyte numbers in 4-week-old Eβ$^{-/-}$ mice vary between 5.0×10^6 and 40×10^6 depending on the individual; Eβ$^{-/-}$ thymuses are comprised of ~55%–65% CD4$^-$ CD8$^-$ thymocytes (of which ~30% are TCRγδ$^+$) and ~35%–45% CD4$^+$ CD8$^+$ thymocytes (of which ~20% are

TCRγδ$^+$); no TCRαβ$^+$ cells are found in Eβ$^{-/-}$ animals (Bouvier et al. 1996; I. Leduc, N. Mathieu and P. Ferrier, unpubl.).

δ$^{-/-}$ Eβ$^{-/-}$ and *rag*$^{-/-}$ Eβ$^{-/-}$ double knockout mice were generated by crossing Eβ$^{-/-}$ males with TCRδ-deficient (δ$^{-/-}$) (Itohara et al. 1993) or RAG1-deficient (*rag*$^{-/-}$) (Spanopoulou et al. 1994) females, respectively, followed by backcrosses of animals carrying both mutations at the heterozygous state to obtain mice homozygous for both. Typically, thymocyte numbers in 4-week-old δ$^{-/-}$ Eβ$^{-/-}$ mice are ≤5.0 × 10^6; δ$^{-/-}$ Eβ$^{-/-}$ thymuses are almost entirely comprised of CD4$^-$ CD8$^-$ thymocytes; no TCRαβ$^+$ or TCRγδ$^+$ cells are found in these animals (I. Leduc, N. Mathieu and P. Ferrier, unpubl.).

Preparation of nuclear templates for in vitro cleavage

Thymuses were harvested from individual *rag*$^{-/-}$ and *rag*$^{-/-}$ Eβ$^{-/-}$ mice. To increase thymic cellularity, these animals had been previously injected with anti-CD3 monoclonal antibodies according to a previously published protocol (Shinkai and Alt 1994). The thymus was disrupted manually into a single cell suspension. Nuclear templates were prepared from thymocytes as described (Parker and Topol 1984) and were shown to be intact by microscopy. Nuclei were resuspended at a final concentration of 50,000/μl in 20 mM HEPES (pH 7.6), 2 mM $MgCl_2$, 70 mM KCl, 0.1 mM EDTA, 1 mM DTT, 0.5 mM PMSF, 25% glycerol and frozen in aliquots at −80°C.

Detection of in vivo-generated SEs by LM-PCR

Genomic DNA (1 μg) purified by standard methods (Ausubel et al. 1987) was ligated to 20 pmoles of BW linker (Mueller and Wold 1989) as described (Schlissel et al. 1993). Ligations were performed in a final volume of 20 μl at 16°C for 12–16 hr. Ligated DNA was diluted with an equal volume of PCR-lysis buffer (10 mM Tris-HCl at pH 8.3, 50 mM KCl, 0.45% NP-40, 0.45% Tween-20) and heated at 95°C for 15 min. Four microliters of the ligated DNA was amplified in each 25-μl PCR reaction. For nested LM-PCR reactions, 12 cycles of amplification were carried out with the distal locus-specific primer and anchor primer *BW-1H* (Schlissel et al. 1993). One microliter of the product was then amplified for another 27 cycles with the proximal locus-specific primer and *BW-1H*. LM-PCR products were separated on a 2% agarose gel (1% SeaKem LE/1% NuSieve) and transferred to a nylon membrane (Hybond N+, Amersham) under alkaline conditions. Filters were prehybridized at 56°C in 6× SSPE, 5× Denhardt's reagent, 0.2% SDS and hybridized with a third locus-specific oligonucleotide in the same solution. A total of 33–50 ng of [γ-^{32}P]ATP end-labeled oligonucleotide was typically hybridized to each Southern blot. Images were generated by use of a PhosphorImager (Molecular Dynamics) and quantitated by use of ImageQuant software (v. 4.1). The identity of specific broken SE LM-PCR products was confirmed either by sequencing (Schlissel et al. 1993) or by restriction enzyme sensitivity (Van Gent et al. 1995) as described. The relative amounts of specific broken DNA ends in different samples were estimated by serially diluting linker-ligated DNA into irrelevant DNA and determining the dilution at which identical hybridization signals were obtained.

In vitro RSS cleavage assays

In vitro cleavage assays were performed exactly as described (Stanhope-Baker et al. 1996). Briefly, each 25-μl reaction contained 100,000 nuclei or 1 μg of purified genomic DNA as the template for cleavage. The template was incubated with 3 μl (~2 μg) of fetal cow thymus nuclear extract (Parker and Topol 1984) and 2 μl of rRAG1 protein (Van Gent et al. 1995) in 40 mM HEPES (pH 7.6), 2.5 mM Tris-Hcl pH 8.0, 110 mM KCl, 1 mM $MnCl_2$, 2.5 mM DTT, 0.2 mM $MgCl_2$, 0.05 mM PMSF, 0.025 mM EDTA, 7% glycerol (vol/vol). Reactions were incubated for 30 min on ice followed by 60 min either on ice or at 30°C. Following this incubation, proteinase buffer (10 mM Tris-HCl at pH 8, 1 mM EDTA, 0.1% SDS) and 20 μg of proteinase K were added, and samples were incubated at 50°C for 1.5–2.0 hr. Samples were then extracted once with phenol/chloroform/isoamyl alcohol (25 : 24 : 1) and once with chloroform/isoamyl alcohol (49 : 1). Nucleic acid was precipitated along with 2 μg of glycogen carrier using NaOAc and ethanol and resuspended in 15–20 μl of deionized H_20. The entire recovered in vitro cleavage reaction product was ligated as described (Schlissel et al. 1993) to 20 pmole of BW linker (Mueller and Wold 1989) for 12–16 hr at 16°C in a volume of 20–25 μl. Control genomic DNAs (1.5 μg) prepared by standard methods (Ausubel et al. 1987) were ligated in parallel. Following ligation, an equal volume of PCR lysis buffer (see above) was added and samples were denatured at 95°C for 15 min. One-twelfth of each sample was typically analyzed in each PCR or LM-PCR reaction. LM-PCR amplification of broken ends generated in vitro was performed with the anchor primer *BW-1H* and a pair of locus-specific primers essentially as described (see above, and Schlissel et al. 1993).

Oligonucleotides used in LM-PCR assays

The sequences (written 5′ to 3′) of the locus-specific oligonucleotide PCR primers and probes used for LM-PCR are listed below. For each assay, the distal primer is listed first, the proximal primer is listed second and the blot hybridization probe is listed third. 5′ of *D*β2 SEs: *Dβ22*, ACCCAGCTTGAGACTTTTCCCAGCC (used as both the distal and the proximal primer); *Dβ25′*, GTAGGCACCTGTGGGGAAGAAACT. 3′ of *D*β2 SEs: *Dβ2R2*, GTTCGTAATTTCCCATGCATGTACG; *Dβ2R1*,GCTGATGGTTAACATGATAAGGGC; *Dβ2R*, GAGTTGGTGTTTTTTTGGGTAG. 5′ of *J*β2.1SEs: *Jβ23*, GAGTGAATAGATGGATATCCGTTC; *Jβ24* CTCCTCCTCAATTTGAGATCGGCC; *Jβ25′ intron*, TATTGAGGAAGGTGAGGAAAGA. 5′ of *J*β2.6 SEs: *Jβ26*, TTCTCTGGGAGTCAGAGGGTTGTGC; *Jβ262* TGATTGGCAGCCGATTGAACAGCCT; *Jβ26H*, GCGTCTTTACCCTGAGTTCCCAAG; 5′ of *J*κ5 SEs: *Jκ1794F*, ACTTGTGACGTTTTGGTTCTG; *Jκ1847F*, GCCATTCCTGGCAACCTGTGCATCA; *Jκ2000F*, TAGTTGGACTGGCTTCACAGGCA.

The sequence of the anchor (linker-specific) primer used for LM-PCR is as follows: *BW-1H*, CCGGGAGATCTGAATTCCAC. The BW linker is composed of oligonucleotides *BW-1* and *BW-2* annealed to one another; *BW-1*, GCGGTGACCCGGGAGATCTGAATTC; *BW-2*, GAATTCAGATC.

The products of control CD14 amplifications (typically 25–30 cycles) were detected by ethidium bromide staining of 1.2% agarose gels. Primers for CD14 amplification were *CD14L*, GCTCAAACTTTCAGAATCTACCGAC, and *CD14R*, AGTCAGTTCGTGGAGGCCGGAAATC.

D*β-to-*J*β signal joint assays*

SJs involving the RSSs 3′ of *D*β2 and 5′ of *J*β2.6 were amplified in a nested PCR reaction. The first round of PCR (12 cycles) was done with primers *Dβ2R2* (see above) and *Jβ1572*, GGCCGGGTTTCTCTGGGAGTC. The primers for the second round of amplification were *Dβ2R1* (see above) and *Jβ1572*. PCR products were extracted once with phenol:chloroform:isoamyl alcohol (25 : 24 : 1) and once with chloroform:isoamyl alcohol (49 : 1). Nucleic acid was precipitated along with 2 μg of glyco-

gen carrier using NaOAc and ethanol and resuspended in 15 µl deionized H_20. One half of the recovered DNA was digested with *Apa*LI (New England BioLabs) at 37°C for 1–4 hr while the other half was incubated with heat-inactivated (65°C for 15 min) *Not*I on ice. The digestion products were separated on agarose gels and transferred to nylon. The filters were hybridized with end-labeled *Dβ2R* (see above). Semi-quantitative analysis of the relative levels of *D*β-to-*J*β SJs in various samples of genomic DNA was performed exactly as described above with dilutions of the template DNA. Template DNA was serially diluted into genomic DNA from a source that does not rearrange TCRβ genes, such as the S107 plasmacytoma cell line. Ku86$^{-/-}$ deficient thymocyte DNA used in Figure 6 was a gift from Dr. M. Nussenzweig (Nussenzweig et al. 1996).

D*β-to-*Jβ *coding joint assays and* Dβ*-to-*Dβ *coding/signal joint assays*

Genomic DNA was diluted to 30 ng/µl in PCR-lysis buffer (see above) and heated to 95°C for 15 min prior to PCR. The primary amplification consisted of 12 cycles each of 94°C for 45 sec, 60°C for 45 sec, and 72°C for 1.5 min with locus-specific primers for the CJ or SJ examined. A second round of PCR was carried out consisting of 27 cycles under the original conditions with 1 µl of the primary PCR product, one nested primer, and the corresponding original primer for each joint examined. For the analysis of CJs, one-third of the amplified DNA was analyzed by electrophoresis on a 1% agarose/0.5% NuSieve gel and blotted as described. The blots were hybridized to [γ-^{32}P] ATP end-labeled locus-specific internal primers and subjected to autoradiography and PhosphorImager analysis. For the analysis of SJs, the amplified DNA was split in half; one-half was digested with *Apa*LI and the other half was mock digested, as described above. The digested and mock-digested DNA was then analyzed exactly as for CJs.

Primers used for the *D*β-to-*J*β CJ assays consisted of *Dβ22* (see above), used for both the primary and the secondary PCR, and *Jβ26R2* (ACCCAATCCCTTTTCATCCCGCTC) for the primary PCR or *Jβ26R1* (TGTCTCCTACTATCGATTTCCCTCC) for the secondary PCR; oligonucleotide *Dβ25′* (see above) was used as the hybridization probe. Primers used for the *D*β1-to-*D*β2 CJ/SJ assays consisted of *Dβ01N* (ACAGGGGTAAAGAGGAAAACCCTG) and *Dβ2R2* (see above) for the primary PCR, *Dβ01N* and *Dβ2R1* (see above) for the secondary PCR, and *Dβ2R* (see above) for the hybridization probe.

Cloning and sequencing of PCR-amplified products

Amplified joints to be sequenced were ligated into P-GEM-T-easy (Promega). Because the vast majority of amplified products represented unrearranged DNA, the *D*β2-to-*J*β2 coding joints from Eβ$^{-/-}$ thymocyte DNA were first separated on a 1.5% agarose gel (1% agarose/0.5% NuSieve) along side the products from wild-type DNA, which were used as a reference. Slices corresponding with the sizes of the two expected products were cut from the gel and the DNA extracted from the agarose by use of the Qiaex II gel extraction kit (Qiagen) according to the manufacturer's instructions. The PCR products for the *D*β1-to-*D*β2 joints generated from Eβ$^{-/-}$ DNA were ligated directly into the vector. In some cases, the PCR products for the *D*β1-to-*D*β2 joints derived from wild-type thymocytes were also ligated directly into the vector. Because there was a large number of signal joints, the PCR products for the *D*β1-to-*D*β2 wild-type joints were also first digested with *Apa*LI to remove the signal joints and then the fragments separated on agarose gels and the DNA extracted as just described, before ligation. This was necessary not only to remove the *Apa*LI cleaved fragments, but also to remove very small products that preferentially ligated into the cloning vector. Small-scale plasmid preparation was performed by standard protocols (Ausubel et al. 1987) and ~100 ng of the DNA was sequenced by use of the Thermo Sequenase radiolabeled terminator cycle sequencing kit (Amersham) and locus-specific primers according to the manufacturer's instructions.

Acknowledgments

We thank M. Malissen for providing the *CD3ϵ* knockout ($\epsilon^{-/-}$) mice and G. Warcollier and M. Pontier for maintaining the mouse colonies. This work was supported by institutional grants from INSERM and CNRS, and by specific grants from the Association pour la Recherche sur le Cancer, the Ministère de la Recherche and the Commission of the European Communities (to P.F.) and from the National Institutes of Health (RO1 AI 40227), the W.W. Smith Charitable Trust, and the Leukemia Society of America (to M.S.). This manuscript was improved by the insightful comments of Drs. S. Desiderio, D. Pardoll, and S. Dillon.

The publication costs of this article were defrayed in part by payment of page charges. This article must therefore be hereby marked ''advertisement'' in accordance with 18 USC section 1734 solely to indicate this fact.

References

Agrawal, A. and D.G. Schatz. 1997. RAG1 and RAG2 form a stable postcleavage synaptic complex with DNA containing signal ends in V(D)J recombination. *Cell* **89:** 43–53.

Alt, F.W., T.K. Blackwell, and G.D. Yancopoulos. 1987. Development of the primary antibody repertoire. *Science* **238:** 1079–1087.

Alt, F.W., E.M. Oltz, F. Young, J. Gorman, G. Taccioli, and J. Chen. 1992. VDJ recombination. *Immunol. Today* **13:** 306–314.

Ausubel, F., R. Brent, R. Kingston, D. Moore, J. Seidman, J. Smith, and K. Struhl. 1987. *Current protocols in molecular biology*. Wiley-Interscience, J. Wiley & Sons, New York.

Blunt, T., D. Gell, M. Fox, G.E. Taccioli, A.R. Lehmann, S.P. Jackson, and P.A. Jeggo. 1996. Identification of a nonsense mutation in the carboxyl-terminal region of DNA-dependent protein kinase catalytic subunit in the scid mouse. *Proc. Natl. Acad. Sci.* **93:** 10285–10290.

Bogue, M.A. and D.B. Roth. 1996. Mechanism of V(D)J recombination. *Curr. Biol.* **8:** 175–180.

Bogue, M.A., C. Wang, C. Zhu, and D.B. Roth. 1997. V(D)J recombination in Ku86-deficient mice: Distinct effects on coding, signal, and hybrid joint formation. *Immunity* **7:** 37–47.

Bories, J.C., J. Demengeot, L. Davidson, and F.W. Alt. 1996. Gene-targeted deletion and replacement mutations of the T-cell receptor β-chain enhancer: The role of enhancer elements in controlling V(D)J recombinational accessibility. *Proc. Natl. Acad. Sci.* **93:** 7871–7876.

Born, W., J. Yagüe, E. Palmer, J. Kappler, and P. Marrack. 1985. Rearrangement of T-cell receptor β-chain genes during T-cell development. *Proc. Natl. Acad. Sci.* **82:** 2925–2929.

Bouvier, G., F. Watrin, M. Naspetti, C. Verthuy, P. Naquet, and P. Ferrier. 1996. Deletion of the mouse T-cell receptor β gene enhancer blocks αβ T-cell development. *Proc. Natl. Acad. Sci.* **93:** 7877–7881.

Candéias, S., C. Waltzinger, C. Benoist, and D. Mathis. 1991. The $V_\beta17^+$ T cell repertoire: Skewed Jβ usage after thymic

selection; dissimilar CDR3s in $CD4^+$ versus $CD8^+$ cells. *J. Exp. Med.* **174:** 989–1000.

Chen, J., F. Young, A. Bottaro, V. Stewart, R.K. Smith, and F.W. Alt. 1993. Mutations of the intronic IgH enhancer and its flanking sequences differentially affect accessibility of the J_H locus. *EMBO J.* **12:** 4635–4645.

Chien, Y.-H., M. Iwashima, D.A. Wettstein, K.B. Kaplan, J.F. Elliott, W. Born, and M.M. Davis. 1987. T-cell receptor δ gene rearrangements in early thymocytes. *Nature* **330:** 722–727.

Constantinescu, A. and M.S. Schlissel. 1997. Changes in locus-specific V(D)J recombinase activity induced by immunoglobulin gene products during B cell development. *J. Exp. Med.* **185:** 609–620.

Danska, J.S., F. Pflumio, C.J. Williams, O. Huner, J.E. Dick, and C.J. Guidos. 1994. Rescue of T cell-specific V(D)J recombination in SCID mice by DNA-damaging agents. *Science* **266:** 450–455.

Danska, J.S., D.P. Holland, S. Mariathasan, K.M. Williams, and C.J. Guidos. 1996. Biochemical and genetic defects in the DNA-dependent protein kinase in murine *scid* lymphocytes. *Mol. Cell. Biol.* **16:** 5507–5517.

Eastman, Q.M., T.M.J. Leu, and D.G. Schatz. 1996. Initiation of V(D)J recombination *in vitro* obeying the 12/23 rule. *Nature* **380:** 85–88.

Errami, A., V. Smider, W.K. Rathmell, D.M. He, E.A. Hendrickson, M.Z. Zdzienicka, and G. Chu. 1996. Ku86 defines the genetic defect and restores X-ray resistance and V(D)J recombination to complementation group 5 hamster cell mutants. *Mol. Cell. Biol.* **16:** 1519–1526.

Friedberg, E.C. 1996. Relationships between DNA repair and transcription. *Annu. Rev. Biochem.* **65:** 15–42.

Gellert, M. 1997. Recent advances in understanding V(D)J recombination. *Adv. Immunol.* **64:** 39–64.

Godfrey, D.I., J. Kennedy, P. Mombaerts, S. Tonegawa, and A. Zlotnik. 1994. Onset of TCR-β gene rearrangement and role of TCR-β expression during $CD3^-CD4^-CD8^-$ thymocyte differentiation. *J. Immunol.* **152:** 4783–4792.

Gorman, J.R., N. van der Stoep, R. Monroe, M. Cogné, L. Davidson, and F.W. Alt. 1996. The Igκ 3′ enhancer influences the ratio of Igκ versus Igλ B lymphocytes. *Immunity* **5:** 241–252.

Hempel, W.M., I. Leduc, N. Mathieu, R.K. Tripathi, and P. Ferrier. 1998. Accessibility control of V(D)J recombination: Lessons from gene targeting. *Adv. Immunol.* (In press).

Hood, L., L. Rowen, and B.F. Koop. 1995. Human and mouse T-cell receptor loci: Genomics, evolution, diversity, and serendipity. *Ann. NY Acad. Sci.* **758:** 390–412.

Itohara, S., P. Mombaerts, J. Lafaille, J. Iacomini, A. Nelson, A.R. Clarkze, M.L. Hooper, A. Farr, et al. 1993. T cell receptor δ gene mutant mice: Independant generation of αβ T cells and programmed rearrangements of γδ TCR genes. *Cell* **72:** 337–348.

Lai, E., R.K. Wilson, and L.E. Hood. 1989. Physical maps of the mouse and human immunoglobulin-like loci. *Adv. Immunol.* **46:** 1–59.

Lauzurica, P. and M.S. Krangel. 1994. Enhancer-dependant and -independant steps in the rearrangement of a human T cell receptor δ transgene. *J. Exp. Med.* **179:** 43–55.

Leu, T.M., Q.M. Eastman, and D.G. Schatz. 1997. Coding joint formation in a cell-free V(D)J recombination system. *Immunity* **7:** 303–314.

Lewis, S.M. 1994. The mechanism of V(D)J joining: Lessons from molecular, immunological, and comparative analyses. *Adv. Immunol.* **56:** 29–150.

Lieber, M.R., J.E. Hesse, S. Lewis, G.C. Bosma, N. Rosenberg, K. Mizuuchi, M.J. Bosma, and M. Gellert. 1988. The defect in murine severe combined immune deficiency: joining of signal sequences but not coding segments in V(D)J recombination. *Cell* **55:** 7–16.

Lieber, M.R., U. Grawunder, X. Wu, and M. Yaneva. 1997. Tying loose ends: Roles of Ku and DNA-dependent protein kinase in the repair of double-strand breaks. *Curr. Opin. Genet. Dev.* **7:** 99–104.

Livak, F. and D.G. Schatz. 1996. T-cell receptor α locus V(D)J recombination by-products are abundant in thymocytes and mature T cells. *Mol. Cell. Biol.* **16:** 609–618.

Malissen, M., A. Gillet, L. Ardouin, G. Bouvier, J. Trucy, P. Ferrier, E. Vivier, and B. Malissen. 1995. Altered T cell development in mice with a targeted mutation of the CD3-ϵ gene. *EMBO J.* **14:** 4641–4653.

McMurry, M.T., C. Hernandez-Munain, P. Lauzurica, and M.S. Krangel. 1997. Enhancer control of local accessibility to V(D)J recombinase. *Mol. Cell. Biol.* **17:** 4553–4561.

Mombaerts, P., A.R. Clarke, M.A. Rudnicki, J. Iacomini, S. Itohara, J.J. Lafaille, L. Wang, Y. Ichigawa, et al. 1992. Mutations in T-cell antigen receptor genes α and β block thymocyte development at different stages. *Nature* **360:** 225–231.

Mueller, P.R. and B. Wold. 1989. In vivo footprinting of a muscle specific enhancer by ligation mediated PCR. *Science* **246:** 780–786.

Nussenzweig, A., C.H. Chen, V.D. Soares, M. Sanchez, K. Sokol, M.C. Nussenzweig, and G.C. Li. 1996. Requirement for Ku80 in growth and immunoglobulin V(D)J recombination. *Nature* **382:** 551–555.

Papavasiliou, F., M. Jankovic, S. Gong, and M.C. Nussenzweig. 1997. Control of immunoglobulin gene rearrangements in developing B cells. *Curr. Opin. Immunol.* **9:** 233–238.

Parker, C.S. and J. Topol. 1984. A Drosophila RNA polymerase II transcription factor contains a promoter-region-specific DNA-binding activity. *Cell* **36:** 357–369.

Ramsden, D.A. and M. Gellert. 1995. Formation and resolution of double-strand break intermediates in *V(D)J* rearrangement. *Genes & Dev.* **9:** 2409–2420.

Ramsden, D.A., T.T. Paull, and M. Gellert. 1997. Cell-free V(D)J recombination. *Nature* **388:** 488–491.

Roth, D.B., P.B. Nakajima, J.P. Menetski, M.J. Bosma, and M. Gellert. 1992. V(D)J recombination in mouse thymocytes: Double-strand breaks near T cell receptor δ rearrangement signals. *Cell* **69:** 41–53.

Roth, D.B., C. Zhu, and M. Gellert. 1993. Characterization of broken DNA molecules associated with V(D)J recombination. *Proc. Natl. Acad. Sci.* 90: 10788–10792.

Schatz, D.G., M.A. Oettinger, and M.S. Schlissel. 1992. V(D)J recombination: Molecular biology and regulation. *Annu. Rev. Immunol.* **10:** 359–383.

Schatz, D.G. 1997. V(D)J recombination moves *in vitro*. *Semin. Immunol.* **9:** 149–159.

Schlissel, M.S. and P. Stanhope-Baker. 1997. Accessibility and the developmental regulation of V(D)J recombination. *Semin. Immunol.* **9:** 161–170.

Schlissel, M.S., A. Constantinescu, T. Morrow, M. Baxter, and A. Peng. 1993. Double-strand signal sequence breaks in *V(D)J* recombination are blunt, 5′-phosphorylated, RAG-dependent, and cell cycle regulated. *Genes & Dev.* **7:** 2520–2532.

Serwe, M. and F. Sablitzky. 1993. V(D)J recombination in B cells is impaired but not blocked by targeted deletion of the immunoglobulin heavy chain intron enhancer. *EMBO J.* **12:** 2321–2327.

Shinkai, Y. and F.W. Alt. 1994. CD3ϵ-mediated signals rescue the development of $CD4^+CD8^+$ thymocytes in $RAG\text{-}2^{-/-}$ mice in the absence of TCR β chain expression. *Int. Immu-*

nol. **6:** 995–1001.

Sleckman, B.P., J.R. Gorman, and F.W. Alt. 1996. Accessibility control of antigen-receptor variable-region gene assembly: Role of *cis*-acting elements. *Annu. Rev. Immunol.* **14:** 459–481.

Spanopoulou, E., C.A. Roman, L.M. Corcoran, M.S. Schlissel, D.P. Silver, D. Nemazee, M.C. Nussenzweig, S.A. Shinton et al. 1994. Functional immunoglobulin transgenes guide ordered B-cell differentiation in RAG-1-deficient mice. *Genes & Dev.* **8:** 1030–1042.

Stanhope-Baker, P., K.M. Hudson, A.L. Shaffer, A. Constantinescu, and M.S. Schlissel. 1996. Cell type-specific chromatin structure determines the targeting of V(D)J recombinase activity in vitro. *Cell* **85:** 887–897.

Steen, S.B., L. Gomelsky, and D.B. Roth. 1996. The 12/23 rule is enforced at the cleavage step of V(D)J recombination *in vivo*. *Genes Cells* **1:** 543–553.

Steen, S.B., L. Gomelsky, S.L. Speidel, and D.B. Roth. 1997. Initiation of V(D)J recombination *in vivo:* Role of recombination signal sequences in formation of single and paired double-strand breaks. *EMBO J.* **16:** 2656–2664.

Van Gent, D.C., J.F. McBlane, D.A. Ramsden, M.J. Sadofsky, J.E. Hesse, and M. Gellert. 1995. Initiation of V(D)J recombination in a cell-free system. *Cell* **81:** 925–934.

Van Gent, D.C., D.A. Ramsden, and M. Gellert. 1996. The RAG1 and RAG2 proteins establish the 12/23 rule in V(D)J recombination. *Cell* **85:** 107–113.

Villey, I., D. Caillol, F. Selz, P. Ferrier, and J.P. De Villartay. 1996. Selective defect in rearrangement of the most 5′ TCR-Jα gene segments evidenced by targeted deletion of the TEA (T early α) element: Implications for regulation of DNA accessibility within the TCR-α locus. *Immunity* **5:** 331–342.

Weaver, D.T. 1995. What to do at an end: DNA double-strand-break repair. *Trends Genet.* **11:** 388–392.

Weis-Garcia, F., E. Besmer, D.J. Sawchuk, W. Yu, Y. Hu, S. Cassard, M.C. Nussenzweig, and P. Cortes. 1997. V(D)J recombination: In vitro coding joint formation. *Mol. Cell. Biol.* **17:** 6379–6385.

Willerford, D.M., W. Swat, and F.W. Alt. 1996. Developmental regulation of V(D)J recombination and lymphocyte differenciation. *Curr. Opin. Genet. Dev.* **6:** 603–609.

Xu, Y., L. Davidson, F.W. Alt, and D. Baltimore. 1996. Deletion of the Igκ light chain intronic enhancer/matrix attachment region impairs but does not abolish VκJκ rearrangement. *Immunity* **4:** 377–385.

Zhong, X.P. and M.S. Krangel. 1997. An enhancer-blocking element between α and β gene segments within the human T cell receptor α/δ locus. *Proc. Natl. Acad. Sci.* **94:** 5219–5224.

Zhu, C. and D.B. Roth. 1995. Characterization of coding ends in thymocytes of *scid* mice: Implications for the mechanism of V(D)J recombination. *Immunity* **2:** 101–112.

Zhu, C.M., M.A. Bogue, D.S. Lim, P. Hasty, and D.B. Roth. 1996. Ku86-deficient mice exhibit severe combined immunodeficiency and defective processing of V(D)J recombination intermediates. *Cell* **86:** 379–389.